J. Biochem. **120**, 946-953 (1996)

Acid and Thermal Unfolding of *Escherichia coli* Dihydrofolate Reductase

Eiji Ohmae,* Toshiyuki Kurumiya,† Shio Makino,† and Kunihiko Gekko*,[1]

**Department of Materials Science and Graduate Department of Gene Science, Faculty of Science, Hiroshima University, Kagamiyama, Higashi-Hiroshima, Hiroshima 739; and †Department of Applied Biological Science, Faculty of Agriculture, Nagoya University, Chikusa-ku, Nagoya, Aichi 464-01*

Received for publication, May 30, 1996

The acid and thermal unfolding of *Escherichia coli* dihydrofolate reductase (DHFR) were studied by means of circular dichroism (CD) and fluorescence spectroscopy. There existed at least one intermediate around pH 4 in the acid unfolding process at 15°C, in which the tertiary structure was disrupted before unfolding of the secondary structure. The fluorescence energy transfer from intrinsic tryptophan residues to 1-anilinonaphthalene-8-sulfonate suggested the disruption of the tertiary structure around some tryptophan residues of the intermediate. The thermal unfolding process at pH 7.0 also involved at least one intermediate having a disrupted tertiary structure and a folded secondary structure. The three-state thermodynamic analysis showed that the intermediate in thermal unfolding was less stable by 1.8 kcal/mol than the native state. The similarity of the far-ultraviolet CD spectra of acid and thermally unfolded forms suggests that both types of unfolding produce the same structure, which may be a molten globule intermediate such as that in the folding kinetics of DHFR. The acid and thermal unfolding were depressed in the presence of KCl due to stabilization of the native form.

Key words: acid unfolding, dihydrofolate reductase, intermediate, molten globule, thermal unfolding.

Dihydrofolate reductase (DHFR) [EC 1.5.1.3] from *Escherichia coli* is a monomeric protein of 159 amino acids with no disulfide bond or prosthetic group. The three-dimensional structure of the enzyme in the crystalline state was determined for the binary DHFR-methotrexate complex (*1*) and recently for the apoenzyme (*2*). The structural characteristics of the enzyme in solution have been extensively studied by many approaches: equilibrium and kinetic unfolding-refolding analyses (*3-5*), two-dimensional NMR spectroscopy (*6, 7*), and enzyme kinetics (*8-10*). However, the conformation of DHFR has remained largely mysterious, *e.g.*, there seem to be at least two conformers with different affinities for cofactor, substrate, and inhibitor (*6-8, 10*). The refolding kinetics from the urea-unfolded state consists of at least six phases including one burst phase (two-types of intermediates and four native or native-like conformers) (*11, 12*). The existence of various conformers and intermediates may be due to the extremely flexible structure of this enzyme as revealed by its large adiabatic compressibility (*13*). Despite the complexity of the refolding kinetics, the equilibrium urea unfolding of DHFR follows a two-state transition model, as revealed by spectroscopic studies such as UV absorption, circular dichroism (CD), and fluorescence spectra (*14*). This is also the case for many mutant DHFRs (*3, 4, 15-20*), although two exceptions are known, V75Y and L28R/E139K (*3, 4*). When guanidine hydrochloride was used as a denaturant, however, the free energy of unfolding was considerably larger than that obtained for urea unfolding, suggesting the binding of chloride ions to DHFR (*18*).

The acid and thermal unfolding of DHFR have been scarcely studied although they are very important for understanding the structural characteristics, stability, and function of this enzyme. Uedaira *et al.* (*21*) and Gekko *et al.* (*18, 19*) showed by differential scanning calorimetry (DSC) that the thermal unfolding of wild-type and some mutant DHFRs follows the three-state model. However, this result was based on irreversible thermograms; and a spectroscopic study under reversible conditions is required for the thermodynamic analysis of thermal unfolding and the characterization of thermally unfolded structure. On the other hand, there is no report on acid unfolding of DHFR. Matters of concern are whether the acid-unfolded structure is same as thermally unfolded one, as found for α-lactalbumin and myoglobin (*22, 23*), and whether the equilibrium molten globule exists in both types of unfolding of DHFR, as found for many small globular proteins (*22-26*). From these viewpoints, we have studied the acid and thermal unfolding of DHFR by means of CD and fluorescence spectroscopy. The structural characteristics of the unfolded and intermediate forms will be discussed in comparison with the refolding kinetic intermediates.

MATERIALS AND METHODS

Protein Purification—DHFR was obtained from *E. coli*

[1] To whom correspondence should be addressed.

Abbreviations: ANS, 1-anilinonaphthalene-8-sulfonate; CD, circular dichroism; DSC, differential scanning calorimetry; DHFR, dihydrofolate reductase.

strain HB101 containing the plasmid pTP64-1, which was 840-fold overexpressed compared to the case of non-plasmid cells for the wild-type protein (*27*). The DHFR protein was purified with a methotrexate-agarose affinity column according to the procedures described previously (*20*). Protein concentration was determined spectrophotometrically using a molar extinction coefficient of 31,100 $M^{-1} \cdot cm^{-1}$ at 280 nm (*8*).

Acid Unfolding—Acid unfolding of DHFR was monitored by circular dichroism (CD) with a Jasco J-720W spectropolarimeter. Temperature of the sample was controlled at 15±0.1°C with a thermobath circulator (NESLAB RTE-110). The protein solution was fully dialyzed against 0.1 mM sodium acetate (pH 8.5) and centrifuged at 14,000 rpm for 20 min to remove the aggregates. The sample solutions with different pHs were prepared by adding a given amount of HCl at a protein concentration of about 20 μM. The pH value of each sample was measured on a pH meter after the spectroscopic measurements.

Acid unfolding was also studied by fluorescence spectroscopy with a Jasco FP-770 spectrofluorometer. The emission spectra on excitation at 290 nm were measured at 300–450 nm and 15±0.1°C at a protein concentration of about 0.5 μM. The width of both the excitation and emission slits was 10 nm. To test the pH dependence of the fluorescence intensity of tryptophan and tyrosine residues, the emission spectra of a mixture of *N*-acetyl-L-tryptophan ethyl ester and *N*-acetyl-L-tyrosine ethyl ester (Aldrich) were measured at various pHs. The molar mixing ratio of two esters was adjusted to 5:4, since a DHFR molecule has five tryptophan and four tyrosine residues. The concentrations of *N*-acetyl-L-tryptophan ethyl ester and *N*-acetyl-L-tyrosine ethyl ester were determined using a molar extinction coefficient of 5,550 $M^{-1} \cdot cm^{-1}$ at 278 nm and 1,340 $M^{-1} \cdot cm^{-1}$ at 274.5 nm in 0.1 M HCl, respectively (*28*). Binding of 1-anilinonaphthalene-8-sulfonate (ANS) to acid-unfolded DHFR was examined by the fluorescence energy transfer from intrinsic tryptophan residues of DHFR to ANS (excitation at 290 nm and emission at 400–550 nm). The ANS concentration was determined using a molar extinction coefficient of 6,800 $M^{-1} \cdot cm^{-1}$ at 370 nm in methanol (*12*). Final concentrations of DHFR and ANS were 1.5 and 1.0 μM, respectively.

Thermal Unfolding—Thermal unfolding of DHFR was monitored by CD spectra with a Jasco J-720W and a Jasco J-40A spectropolarimeters. Protein concentration was kept at about 5 μM for the CD measurement at 222 nm and about 20 μM for that at 290 nm. The buffer used was 10 mM potassium phosphate (pH 7.0) containing 0.1 mM dithiothreitol and 0.1 mM EDTA. For comparison, the temperature dependence of CD and fluorescence was also examined at pH 2.5, employing a buffer of 0.1 mM sodium acetate and HCl. The pH values of the sample solutions were adjusted at 25°C before heating. The sample solution was introduced into a quartz cell with 5-mm light path and the temperature was elevated in steps of about 2°C by circulating water of a given temperature through the cell housing with a thermobath circulator (NESLAB RTE-110). The temperature of the sample was measured within an accuracy of ±0.1°C using a digital thermometer (Takara Kogyo, D221), which was connected to a sensor set in the top part of the sample solution. The ellipticity at each temperature was read as an equilibrium value 15 min after each temperature change. To protect the protein from ultraviolet irradiation, the slit on the polarimeter was closed during the intervals of temperature changing, and opened for 60-90 s to read the ellipticity at each temperature (*29*).

Thermal unfolding of DHFR was also monitored by fluorescence spectra with a Jasco FP-770 spectrofluorometer. The emission spectra at 300-450 nm on exciting at 290 nm was measured as a function of temperature. The sample conditions were same as those for CD measurements except for the protein concentration, 0.5 μM.

Effect of KCl—To investigate the salt-binding effect on the DHFR stability, various concentrations of KCl were added to the sample solutions. The conditions of spectroscopic measurements were same as described above.

RESULTS

Acid Unfolding—Figure 1 shows the far-ultraviolet CD and fluorescence spectra of DHFR at various pHs and 15°C. As shown in Fig. 1A, the CD spectra of DHFR at pH 5.7 and 4.1 were almost same as that at pH 7.0, although the molar ellipticity was slightly smaller around 230 nm and larger around 210 nm. On the other hand, the CD spectra largely changed at pH 3.1 and 2.5, indicating that the secondary structure of DHFR was unfolded under acidic conditions.

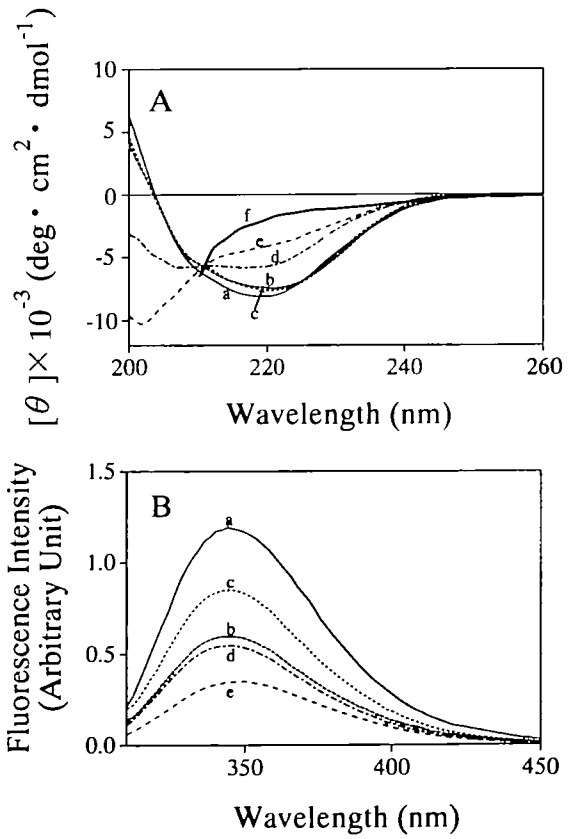

Fig. 1. Circular dichroism (A) and fluorescence (B) spectra of DHFR at 15°C and various pH. The solvent was 0.1 mM sodium acetate and pH was adjusted with HCl. (A) (—, a) pH 7.0; (– –, b) pH 5.7; (·····, c) pH 4.1; (·–·–·, d) pH 3.1; (– – –, e) pH 2.5; (—, f) 6 M urea at pH 7.0. (B) (—, a) pH 7.0; (– –, b) pH 4.8; (·····, c) pH 4.1; (·–·–·, d) pH 3.0; (– – –, e) pH 2.5.

However, the fact that the molar ellipticity at 222 nm and pH 2.5, $-4{,}500$ deg·cm²·dmol^{-1}, is obviously smaller than that in 6 M urea solution, $-1{,}600$ deg·cm²·dmol^{-1} (*20*), means that there exists some residual secondary structure in the acid-unfolded form of DHFR. The near-ultraviolet CD spectrum of acid-unfolded form was not successfully measured because of its low solubility. Then the tertiary structure at low pH was studied by fluorescence spectroscopy.

As shown in Fig. 1B, the pH dependence of the fluorescence spectra is not simple. The fluorescence intensity decreased on decreasing pH from 7.0 to 4.8, followed by an increase at pH 4.1, then again decreased in the lower pH region where the large CD change was observed. The peak wavelengths of the spectra were 345, 345, 346, 349, and 353 nm at pH 7.0, 4.8, 4.1, 3.0, and 2.5, respectively. These results suggest that the tertiary structure of DHFR may loosen before the secondary structure unfolds in the low pH region. The peak wavelength at pH 2.5, 353 nm, is considerably lower than that for the mixture of *N*-acetyl-L-tryptophan ethyl ester and *N*-acetyl-L-tyrosine ethyl ester, 365 nm, at pH 2.5-7.0 (data not shown). This result suggests that the aromatic amino acid residues are not completely exposed to the solvent, as expected by the residual secondary structure.

Figure 2 shows the pH dependence of the molar ellipticity at 222 nm and the fluorescence intensity at 345 nm of DHFR at 15°C. As revealed by the ellipticity data, the secondary structure starts unfolding around pH 3.5 and the most unfolded state appears at pH 2.5-2.8. Lowering pH below 2.5 brought about refolding of the secondary structure, probably due to the increased chloride ions in the medium, as discussed below. Interestingly, the fluorescence intensity increased remarkably in the pH range of 5 to 4, where the secondary structure remains folded. This fluorescence change is not due to the aggregation of DHFR, its isoelectric point being 4.7, because the normalized intensity did not depend on the DHFR concentration. Since the fluorescence intensity of the mixture of *N*-acetyl-L-tryptophan ethyl ester and *N*-acetyl-L-tyrosine ethyl ester was constant in the pH range of 7 to 3, the pH effects on the tryptophan and tyrosine fluorescence can be neglected. Thus the enhanced fluorescence of DHFR around pH 4 could be ascribed to the conformational change of DHFR associated with the exposure of a part of these residues to the solvent.

To confirm this, we measured the energy transfer from the tryptophan residues of DHFR to 1-anilinonaphthalene-8-sulfonate (ANS). Figure 3 shows the fluorescence emission spectra of ANS at 15°C, which were induced by its binding to DHFR at pH 6.1, 3.9, and 2.4. There was no detectable spectrum in the wavelength region of 450 to 500

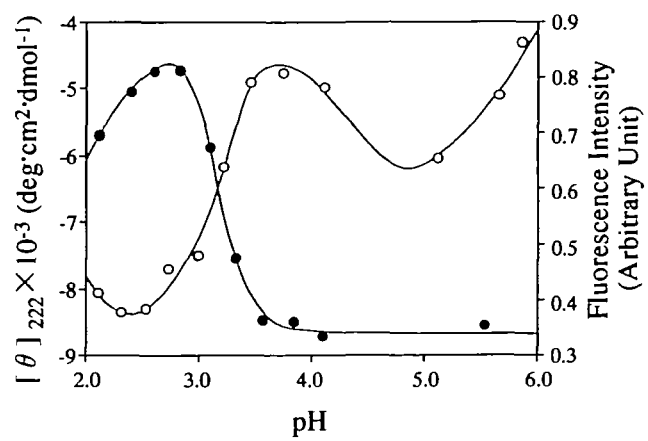

Fig. 2. **pH dependence of the CD and fluorescence intensity of DHFR at 15°C.** The solvent was 0.1 mM sodium acetate and pH was adjusted with HCl. The molar ellipticity (●) was monitored at 222 nm and the fluorescence intensity (○) was monitored at 345 nm on excitation at 290 nm. The lines were drawn by inspection.

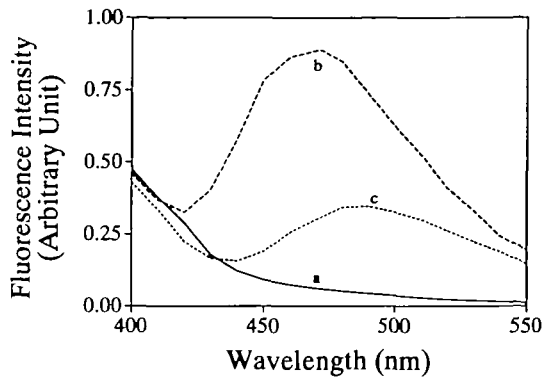

Fig. 3. **1-Anilinonaphthalene-8-sulfonate (ANS) emission spectra induced by the binding to DHFR at 15°C.** The excitation wavelength was 290 nm. The solvent was 0.1 mM sodium acetate and pH was adjusted with HCl. The concentrations of DHFR and ANS were 1.5 and 1.0 μM, respectively. (—, a) pH 6.1; (----, b) pH 3.9; (··, c) pH 2.5.

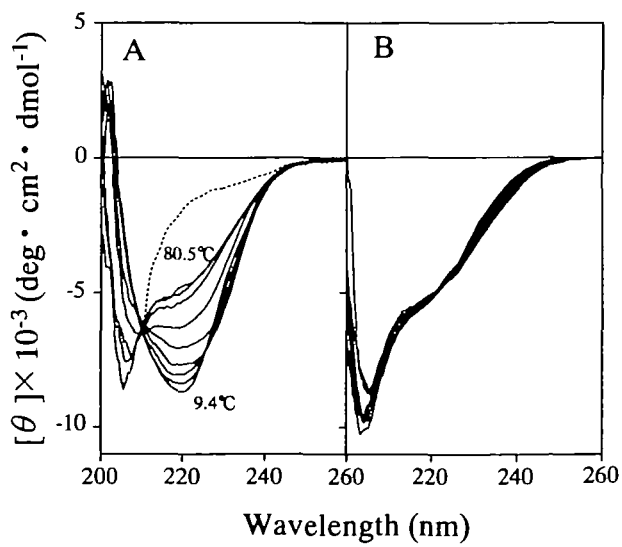

Fig. 4. **Temperature dependence of the far-ultraviolet CD spectra of DHFR at pH 7.0 (A) and 2.5 (B).** (A) The solvent was 10 mM potassium phosphate (pH 7.0) containing 0.1 mM EDTA and 0.1 mM dithiothreitol. The spectra from bottom to top refer to the temperatures 9.4, 18.4, 27.1, 35.9, 44.7, 52.3, 61.9, 70.2, and 80.5°C. A broken line indicates a spectrum in 6 M urea solution at 15°C. (B) The solvent was 0.1 mM sodium acetate containing HCl (pH 2.5). The spectra were measured at 12.8, 18.4, 26.5, 34.5, 43.7, 53.0, 61.6, 70.7, and 78.1°C.

nm at pH 6.1, indicating that the tryptophan residues of native DHFR were essentially not exposed to the solvent. When the ANS concentration was increased to 50 μM, however, a small emission spectrum having a peak at 474 nm appeared at pH 6.1 (data not shown). Therefore, ANS could weakly bind to the native form of DHFR, as suggested by Jones *et al.* (*12*). On the other hand, a large emission spectrum with a peak at 472 nm was observed at pH 3.9, suggesting that ANS would bind to the hydrophobic site near some tryptophan residues partly exposed to the solvent. A small emission spectrum was also observed at pH 2.4 but its peak wavelength, 485 nm, was considerably higher than that at pH 3.9. This indicates that ANS could bind to the acid-unfolded DHFR but the binding sites may be more solvent-accessible as compared with those at pH 3.9.

Thermal Unfolding—Figure 4 shows the far-ultraviolet CD spectra of DHFR at various temperatures at pH 7.0 (A) and 2.5 (B). These spectra demonstrate that the thermal unfolding is induced at pH 7.0 but not at pH 2.5, where the spectra are almost independent of temperature. The molar ellipticity at 222 nm, $-4{,}500$ deg·cm^2·dmol^{-1}, at pH 7.0 and 80°C, was smaller than that in 6 M urea solution, indicating the residual secondary structure in the thermally unfolded form as well as the acid-unfolded form of DHFR. This is supported by the findings that the fluorescence peak wavelength, 352 nm, at pH 7.0 and 80°C, is shorter than that of the mixture of *N*-acetyl-L-tryptophan ethyl ester and *N*-acetyl-L-tyrosine ethyl ester, 365 nm. A noteworthy point is that the CD spectra and the fluorescence peak wavelength at pH 7.0 and 80°C are essentially same as those of the acid-unfolded form at pH 2.5 and 15°C. These results strongly suggest that the acid and thermally unfolded forms of DHFR have the same structure, as found for some other proteins (*22, 23*).

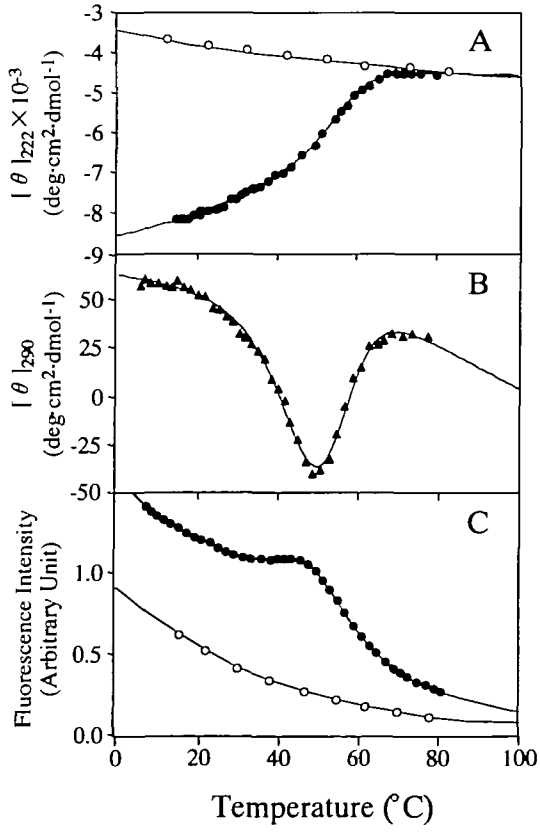

Fig. 5. **Temperature dependence of the CD at 222 nm (A) and 290 nm (B), and fluorescence intensity (C) of DHFR at pH 7.0 and 2.5.** The solvents used were 10 mM potassium phosphate (pH 7.0) containing 0.1 mM EDTA and 0.1 mM dithiothreitol, and 0.1 mM sodium acetate containing HCl (pH 2.5). (A) (●) pH 7.0; (○) pH 2.5. The solid line attached to closed circles represents the theoretical fits to the three-state model. The line attached to open circles was drawn by inspection. (B) pH 7.0. The solid line represents the theoretical fits to the three-state model. (C) (●) pH 7.0; (○) pH 2.5. Each solid line was drawn by inspection.

Figure 5 shows the temperature dependence of the molar ellipticity at 222 nm (A) and 290 nm (B), and the fluorescence intensity at 344 nm (C) of DHFR at pH 7.0 and 2.5. Evidently, there was no thermal transition at pH 2.5, as revealed by a monotonous decrease in the CD and fluorescence intensities (Fig. 5, A and C). A considerably large decrease in fluorescence intensity with temperature was not due to the structural change of DHFR but due to the temperature dependence of the tryptophan and tyrosine fluorescence (*30*). As shown in Fig. 5A, on the other hand, a thermal unfolding of the secondary structure occurred at pH 7.0 in the temperature range of 30-70°C, which involved the major transition in the range of 45 to 60°C. The CD at 290 nm (Fig. 5B) and the fluorescence intensity (Fig. 5C) also showed the thermal transition or the disruption of tertiary structure in the same temperature region. However, both figures obviously show the two-phase transition in the temperature regions of 20-50 and 50-70°C. The second transition at higher temperature seems to correspond to the major transition observed by the CD at 222 nm (Fig. 5A). The peak wavelengths of the fluorescence spectra were 345, 346, and 352 nm at 15, 45, and 80°C, respectively (data not shown). These results indicate that the tertiary structure disrupts at the lower temperature region prior to the global unfolding of the secondary structure, and at least one intermediate with a native-like secondary structure and a disrupted tertiary structure exists in the thermal unfolding process of DHFR at pH 7.0. The existence of the intermediate was also suggested by DSC in the previous studies (*18, 21*).

The reversibility of thermal unfolding was more than 95% under these experimental conditions, judging from the recovery of the molar ellipticity after cooling. This allows us to evaluate the thermodynamic parameters for unfolding. The observed molar ellipticity data, $[\theta]$, were fitted to the three-state unfolding model, native (N) ⇌ intermediate (I) ⇌ unfolded (U), by means of a nonlinear least-squares

TABLE I. **Thermodynamic parameters for thermal unfolding of DHFR at pH 7.0.**[a]

	N⇌I	I⇌U	N⇌U[b]
$\Delta G°$ at 15°C (kcal/mol)	1.8	1.9	3.7[c]
T (°C)[d]	45.0	53.0	49.4 (49.3[e])

[a]The solvent used was 10 mM potassium phosphate containing 0.1 mM EDTA and 0.1 mM dithiothreitol. The thermodynamic parameters were calculated using the $[\theta]$ data points at 222 and 290 nm (see the text for details). [b]N, I, and U represent the native, intermediate, and unfolded form, respectively. [c]The $\Delta G°$ value for N⇌U was calculated as the sum of the $\Delta G°$ values for N⇌I and I⇌U. [d]Mid-point temperature of each transition at which $\Delta G° = 0$. [e]The value in parenthesis shows the result of DSC (*18*).

regression analysis with a SALS program (*31*), as follows

$$[\theta] = [\theta]_N f_N + [\theta]_I f_I + [\theta]_U f_U \quad (1)$$

where $[\theta]_N$, $[\theta]_I$, and $[\theta]_U$ are the molar ellipticities of the native, intermediate, and unfolded forms, respectively, and f_N, f_I, and f_U the population of each form. $[\theta]_N$, $[\theta]_I$, and $[\theta]_U$ at a given temperature were estimated by assuming them to be linearly temperature-dependent. The populations, f_N, f_I, and f_U were calculated as follows

$$f_N = 1/(1 + K_1 + K_1K_2) \quad (2a)$$

$$f_I = K_1/(1 + K_1 + K_1K_2) \quad (2b)$$

$$f_U = K_1K_2/(1 + K_1 + K_1K_2) \quad (2c)$$

where K_1 and K_2 are the equilibrium constants for the reactions N⇌I and I⇌U, respectively. K_1 and K_2 were calculated from the Gibbs free energy change corresponding to each reaction as follows

$$K_n = \exp(-\Delta G^\circ_n/RT) \quad (3)$$

where n is 1 or 2, R the gas constant, and T the absolute temperature. Finally, the temperature dependence of the free energies was estimated assuming the following equation with the fitting parameters a_n, b_n, and c_n.

$$\Delta G^\circ_n = a_nT^2 + b_nT + c_n \quad (4)$$

The Gibbs free energy change between the native and unfolded forms, ΔG°_t, was calculated as the summation of ΔG°_1 and ΔG°_2 at a given temperature. The transition temperatures of each unfolding process, T_n, were calculated as the solution of $\Delta G^\circ_n = 0$.

Table I shows the Gibbs free energy change of unfolding, ΔG°_n, at 15°C and the corresponding transition temperature, T_n. These results were calculated by fitting simultaneously the $[\theta]$ data points at 222 and 290 nm to the above equations. The fluorescence data were not used for fitting because the temperature dependence of the base-line seemed not to be linearly dependent on the temperature. Although the calculation errors of fitting parameters were large, the transition temperature from native to unfolded form, 49.4°C, is consistent with that obtained by the DSC experiment, 49.3°C (*18*). The Gibbs free energy change from native to unfolded form, 3.7 kcal/mol, is also reasonable, considering that the ΔG° value for urea unfolding is 6.08 kcal/mol at this temperature (*19*) and the thermally unfolded form has more residual structure than the urea-unfolded one.

Effect of KCl—Figure 6 shows the far-ultraviolet CD spectra at pH 5.7 (A), 3.1 (B), and 2.5 (C) in the presence or absence of KCl. As shown in Fig. 6A, the spectrum was only slightly modified by adding KCl at neutral pH. But the spectra at pH 3.1 and 2.5 recovered in the presence of KCl to that of the native state at pH 5.7 (Fig. 6, B and C). These results clearly indicate that DHFR was refolded by addition of KCl under the acidic conditions.

Figure 7 shows the pH dependence of the intrinsic

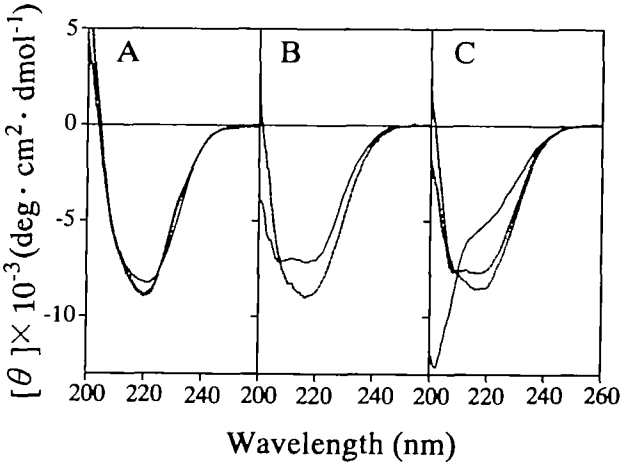

Fig. 6. **Effect of KCl on the far-ultraviolet CD spectra of DHFR at pH 5.7 (A), 3.1 (B), and 2.5 (C).** The solvent was 0.1 mM sodium acetate and pH was adjusted with HCl. (A) (—) without KCl; (----) 0.08 M KCl; (··· ·) 0.3 M KCl. (B) (—) without KCl; (----) 0.08 M KCl. (C) (—) without KCl; (----) 0.08 M KCl; (·····) 0.2 M KCl.

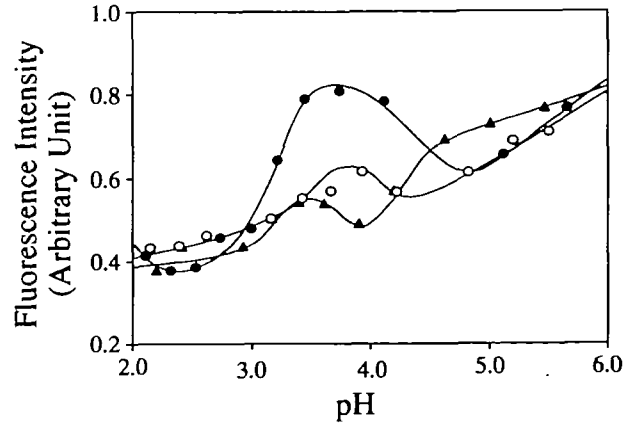

Fig. 7. **Effect of KCl on the fluorescence intensity at 15°C.** The fluorescence intensity was monitored at 345 nm on exciting at 290 nm. The solvent was 0.1 mM sodium acetate and pH was adjusted with HCl. (●) without KCl; (○) 0.04 M KCl; (▲) 0.10 M KCl. The solid lines were drawn by inspection.

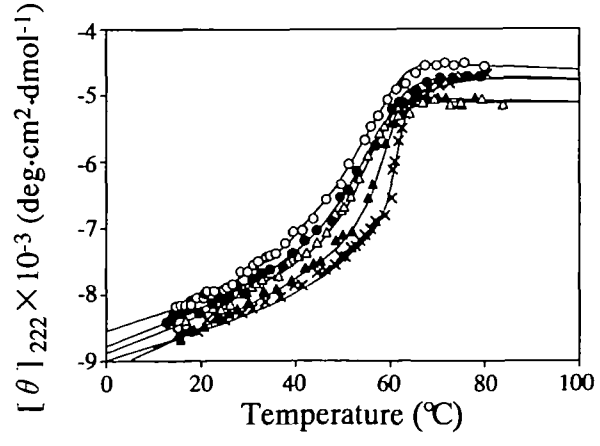

Fig. 8. **Effect of KCl on the CD at 222 nm and pH 7.0.** The solvent was 10 mM potassium phosphate containing 0.1 mM EDTA and 0.1 mM dithiothreitol. (○) without KCl; (●) 0.01 M KCl; (△) 0.05 M KCl; (▲) 0.10 M KCl; (×) 0.42 M KCl. The solid lines attached to each symbol were drawn by the least-squares methods assuming the three-state model.

tryptophan fluorescence monitored at 345 nm in the presence or absence of KCl. The large peak intensity at pH 3.5-4.0 without KCl, caused by the acid-unfolding intermediate, was depressed by addition of KCl, suggesting that the population of the intermediate decreases and the native form is stabilized in the presence of KCl.

Figure 8 shows the temperature dependence of the molar ellipticity at 222 nm of DHFR at various concentrations of KCl. As the KCl concentration was increased, the transition temperature was elevated and the cooperativity of the transition was enhanced. The transition curve essentially followed the two-state model at 0.10 and 0.42 M KCl. These results also demonstrate that the native form was stabilized by addition of KCl.

DISCUSSION

Structure of Acid and Thermally Unfolded Forms—The acid unfolding of DHFR was investigated for the first time in the present study. The structure of the acid-unfolded form has a considerable amount of residual secondary structure as revealed by the molar ellipticity of $-4{,}500$ deg·cm^2·dmol^{-1} at 222 nm. This is also supported by a fluorescence spectroscopy: the peak wavelength, 353 nm, is lower than that for the urea-unfolded form, 365 nm, and only small fluorescence is induced by binding ANS. These results are very similar to those found for the thermally unfolded DHFR, indicating that the acid and thermally unfolded forms have the same secondary and tertiary structures. That the acid-unfolded DHFR shows no structural change on heating (Figs. 4B and 5C) suggests the absence of cooperative heat absorption in DSC experiment, which is one of the typical characteristics of a molten globule (*22, 23, 32, 33*). Therefore, the acid and thermally unfolded forms of DHFR could be regarded as having the molten globule structure. Equilibrium molten globules have been detected for many proteins under acidic conditions (*22, 23, 25, 26*).

It is interesting that the structures of the acid and thermally unfolded forms are identical even though the driving force of the unfolding is different. Acid unfolding is caused by the electrostatic repulsion of the positively charged groups due to proton binding to the carboxyl groups. On the other hand, thermal unfolding is mainly induced by the enhanced thermal fluctuation overcoming the stabilizing forces such as hydrogen bonds and van der Waals interaction. The fact that these different sources produce the same unfolded form means that this form is one of the energetically minimum structures of DHFR, whose formation does not depend on the pathway.

Structure of Intermediates in Acid and Thermal Unfolding—The acid-unfolding process of DHFR involves at least one intermediate in which the secondary structure remains native but the tertiary structure is disrupted, as revealed by the absence of a detectable CD change at 222 nm and the largely induced fluorescence (Figs. 1 and 2). The ANS binding to the intermediate also supported the exposure of some hydrophobic surface accompanying a disruption of the tertiary structure (Fig. 3). Since we measured the energy transfer from the intrinsic tryptophan residues to ANS, this disruption may include a structural change around some tryptophan residues. A possibility is the breakdown of the exciton pair of tryptophan-47 and tryptophan-74. Kuwajima *et al.* (*5*) reported that these tryptophans make an exciton coupling in the native DHFR and the disruption of this exciton causes the approximately equivalent increase and decrease in CD intensity at 220 and 230 nm, respectively. This feature was observed for the CD spectra on changing pH 7.0 to pH 4.1 (Fig. 1A), suggesting that this exciton pair may be disrupted in the intermediate of acid unfolding of DHFR.

The DSC deconvolution analysis predicted that the thermal unfolding of DHFR involves one intermediate at neutral pH, although its structure was not definitely characterized (*18, 21*). The existence of the intermediate was confirmed spectrophotometrically in the present study. The intermediate has the native-like secondary structure with a disrupted tertiary structure, as revealed by the near-ultraviolet CD and fluorescence intensities and the lack of a detectable CD change at 222 nm. The CD spectra at low temperatures showed an isoellipticity point at 225 nm and the approximately equal increase and decrease in CD intensity at the shorter and longer wavelength, respectively (Fig. 4A). This result may also be evidence for the disruption of tryptophan-47 and tryptophan-74 exciton pair in the intermediate of thermal unfolding. As shown by the thermodynamic analysis (Table I), the intermediate is a middle structure, which is less stable by 1.8 kcal/mol than the native state and more stable by 1.9 kcal/mol than the thermally unfolded state in a free energy level, while it was rather close to the native state in its enthalpy level (*34*).

As mentioned above, the intermediates in the acid and thermal unfolding processes have similar characteristics. 1: Both intermediates have the native-like secondary structure and the disrupted tertiary structure. 2: The tryptophan-47 and tryptophan-74 exciton pair may be disrupted. 3: The fluorescence spectra have the same peak wavelength at 346 nm. 4: The acid-unfolding intermediate has a high aggregation property as seen in the thermal unfolding process. A noteworthy difference between the intermediates is that the thermal unfolding intermediate had no ANS binding ability while the acid-unfolding intermediate did. The ANS fluorescence was not induced in the thermal unfolding process even when the ANS concentration was 100-fold higher than that used for the acid-unfolding process (data not shown). Thus, both intermediates have a similar secondary structure, but the tertiary structure of the acid-unfolding intermediate may be more largely disrupted than that of the thermal unfolding intermediate.

Comparison with Folding Kinetics—Recent kinetic studies of DHFR have shown that there exist at least six (one burst and five measurable) phases in the folding reaction from the urea-unfolded form (*11, 12*). The burst-phase intermediate is known to have some characteristics of a molten globule. The molar ellipticity of the burst-phase intermediate was estimated to be about $-5{,}000$ deg·cm^2·dmol^{-1} at 220 nm by the stopped-flow CD experiments (*5*). This intermediate can bind ANS but it does not induce the fluorescence as strongly as does the second (native-like) intermediate (*12*). These results are very similar to those found for the acid and thermally unfolded DHFRs in the present study. Therefore, we may expect that the acid and thermally unfolded forms of DHFR have the molten globule structure, which corresponds to the burst-phase intermedi-

ate found in the folding kinetics. The similarity of the acid-unfolded form and the folding kinetic intermediate has been confirmed for α-lactalbumin and apomyoglobin (*35, 36*).

The five measurable phases have some native-like structure in which the exciton pair of tryptophan-47 and tryptophan-74 is established (*11*). However, the fastest measurable intermediate has some specific features compared to the other four measurable phases, such as the strong inducement of the ANS fluorescence (*12*) and the inability to bind the inhibitor methotrexate (*11, 14*). As shown in Fig. 3, the acid-unfolding intermediate strongly induced the fluorescence of ANS. We have also found preliminarily that methotrexate is not stoichiometrically bound to DHFR at acidic pHs. These findings suggest that the acid-unfolding intermediate has a similar structure to the fastest measurable phase intermediate in the folding kinetics, while the tryptophan-47 and tryptophan-74 exciton pair seems to be disrupted in the intermediates of acid and thermal unfolding processes (Figs. 1A and 4A). More detailed experiments would be necessary for comparative discussion of the acid and thermal unfolding intermediates with the kinetic intermediates.

Effect of KCl—As shown in Figs. 7 and 8, the intermediates in the acid and thermal unfolding processes were diminished and the native state was stabilized by addition of KCl. The similar structural stabilization by KCl was also observed for the urea unfolding (*18*). These KCl effects may be ascribed to two possible origins: an increased ionic strength, and the specific binding of potassium and/or chloride ions. The addition of NaCl had a similar effect to KCl but the addition of 0.03 M Na_2SO_4, which has comparable ionic strength to 0.1 M KCl, had no effect on the thermal unfolding of DHFR (data not shown). Thus, the specific binding of chloride ions is the most reasonable explanation for the KCl-induced refolding or the stabilization of the native state of DHFR. X-ray crystallographic data also suggested a binding site for chloride ions in the DHFR molecule (*1, 2*). Thus refolding of acid-unfolded DHFR with HCl below pH 2.5 (Fig. 2) could be ascribed to the binding effect of chloride ions. Recently Fink *et al.* (*26*) reported that chloride ions can cause refolding from the acid-unfolded state to the molten globule state for several proteins. DHFR might belong to such a category of proteins.

As demonstrated in this study, *E. coli* DHFR is easily unfolded by acid or heat, with one intermediate in each unfolding process. Chloride ions have a stabilizing effect on the native structure in both types of unfolding as well as urea unfolding. The unfolded structure by acid and heat is essentially the same and can be regarded as the molten globule, which corresponds to the burst-phase intermediate in the folding kinetics. The intermediate in acid unfolding may be a structure close to the second intermediate observed in the folding kinetics. Further insight into the characteristics of the intermediates is expected from a study, now in progress, on the acid and thermal unfolding of mutant DHFRs.

We wish to thank Dr. M. Iwakura of the National Institute of Bioscience and Human Technology for the gift of plasmid pTP64-1 and for helpful discussions. We also thank Prof. K. Yoshikawa of Nagoya University for the use of the J-720W spectropolarimeter and Prof. M. Isobe of Nagoya University for the use of the FP-770 spectrofluorometer. We also thank the Nagoya University Computer Center for the use of the SALS program.

REFERENCES

1. Bolin, J.T., Filman, D.J., Matthews, D.A., Hamlin, R.C., and Kraut, J. (1982) Crystal structures of *Escherichia coli* and *Lactobacillus casei* dihydrofolate reductase refined at 1.7 Å resolution. *J. Biol. Chem.* **257**, 13650-13662
2. Bystroff, C. and Kraut, J. (1991) Crystal structure of unliganded *Escherichia coli* dihydrofolate reductase: Ligand-induced conformational changes and cooperativity in binding. *Biochemistry* **30**, 2227-2239
3. Garvey, E.P. and Matthews, C.R. (1989) Effects of multiple replacements at a single position on the folding and stability of dihydrofolate reductase from *Escherichia coli*. *Biochemistry* **28**, 2083-2093
4. Perry, K.M., Onuffer, J.J., Gittelman, M.S., Barmat, L., and Matthews, C.R. (1989) Long-range electrostatic interactions can influence the folding, stability, and cooperativity of dihydrofolate reductase. *Biochemistry* **28**, 7961-7968
5. Kuwajima, K., Garvey, E.P., Finn, B.E., Matthews, C.R., and Sugai, S. (1991) Transient intermediates in the folding of dihydrofolate reductase as detected by far-ultraviolet circular dichroism spectroscopy. *Biochemistry* **30**, 7693-7703
6. Birdsall, B., Feeney, S.J.B., Tendler, S.J., Hammond, D.J., and Roberts, G.C.K. (1989) Dihydrofolate reductase: Multiple conformations and alternative modes of substrate binding. *Biochemistry* **28**, 2297-2305
7. Falzone, C.J., Wright, P.E., and Benkovic, S.J. (1991) Evidence for two interconverting protein isomers in the methotrexate complex of dihydrofolate reductase from *Escherichia coli*. *Biochemistry* **30**, 2184-2191
8. Fierke, C.A., Johnson, K.A., and Benkovic, S.J. (1987) Construction and evaluation of the kinetic scheme associated with dihydrofolate reductase from *Escherichia coli*. *Biochemistry* **26**, 4085-4092
9. Howell, E.E., Booth, C., Farnum, M., Kraut, J., and Warren, M.S. (1990) A second-site mutation at phenylalanine-137 that increases catalytic efficiency in the mutant aspartate-27→serine *Escherichia coli* dihydrofolate reductase. *Biochemistry* **29**, 8561-8569
10. Li, L. and Benkovic, S.J. (1991) Impact on catalysis of secondary structure manipulation of the αC-helix of *Escherichia coli* dihydrofolate reductase. *Biochemistry* **30**, 1470-1478
11. Jennings, P.A., Finn, B.E., Jones, B.E., and Matthews, C.R. (1993) Reexamination of the folding mechanism of dihydrofolate reductase from *Escherichia coli*: Verification and refinement of a four-channel model. *Biochemistry* **32**, 3783-3789
12. Jones, B.E., Jennings, P.A., Pierre, R.A., and Matthews, C.R. (1994) Development of nonpolar surfaces in the folding of *Escherichia coli* dihydrofolate reductase detected by 1-anilinonaphthalene-8-sulfonate binding. *Biochemistry* **33**, 15250-15258
13. Gekko, K., Tamura, Y., Ohmae, E., Hayashi, H., Kagamiyama, H., and Ueno, H. (1996) A large compressibility change of protein induced by a single amino acid substitution. *Protein Sci.* **5**, 542-545
14. Touchette, N.A., Perry, K.M., and Matthews, C.R. (1986) Folding of dihydrofolate reductase from *Escherichia coli*. *Biochemistry* **25**, 5445-5452
15. Perry, K.M., Onuffer, J.J., Touchette, N.A., Herndon, C.S., Gittelman, M.S., Matthews, C.R., Chen, J.T., Mayer, R.J., Taira, K., Benkovic, S.J., Howell, E.E., and Kraut, J. (1987) Effect for single amino acid replacements on the folding and stability of dihydrofolate reductase from *Escherichia coli*. *Biochemistry* **26**, 2674-2682
16. Ahrweiler, P.M. and Frieden, C. (1991) Effects of point mutations in a hinge region on the stability, folding, and enzymatic activity of *Escherichia coli* dihydrofolate reductase. *Biochemistry* **30**, 7801-7809
17. Texter, F.L., Spencer, D.B., Rosenstein, R., and Matthews, C.R. (1992) Intramolecular catalysis of a proline isomerization reac-

tion in the folding of dihydrofolate reductase. *Biochemistry* **31**, 5687-5691
18. Gekko, K., Yamagami, K., Kunori, Y., Ichihara, S., Kodama, M., and Iwakura, M. (1993) Effects of point mutations in a flexible loop on the stability and enzymatic function of *Escherichia coli* dihydrofolate reductase. *J. Biochem.* **113**, 74-80
19. Gekko, K., Kunori, Y., Takeuchi, H., Ichihara, S., and Kodama, M. (1994) Point mutations at glycine-121 of *Escherichia coli* dihydrofolate reductase: Important roles of a flexible loop in the stability and function. *J. Biochem.* **116**, 34-41
20. Ohmae, E., Iriyama, K., Ichihara, S., and Gekko, K. (1996) Effects of point mutations at the flexible loop glycine-67 of *Escherichia coli* dihydrofolate reductase on its stability and function. *J. Biochem.* **119**, 703-710
21. Uedaira, H., Kidokoro, S., Iwakura, M., Honda, S., and Ohashi, S. (1990) Thermal transition of a mutated dihydrofolate reductase. *Thermochim. Acta* **163**, 123-128
22. Griko, Y.V., Friere, E., and Privalov, P.L. (1994) Energetics of the α-lactalbumin states: A calorimetric and statistical thermodynamic study. *Biochemistry* **33**, 1889-1899
23. Griko, Y.V., Privalov, P.L., Venyaminov, S.Y., and Kutyshenko, V.P. (1988) Thermodynamic study of the apomyoglobin structure. *J. Mol. Biol.* **202**, 127-138
24. Hua, Q.X., Ladbury, J.E., and Weiss, M.A. (1993) Dynamics of a monomeric insulin analogue: Testing the molten-globule hypothesis. *Biochemistry* **32**, 1433-1442
25. Goto, Y. and Fink, A.L. (1989) Conformational states of beta-lactamase: Molten-globule states at acidic and alkaline pH with high salt. *Biochemistry* **28**, 945-952
26. Fink, A.L., Calciano, L.J., Goto, Y., Kurotsu, T., and Palleros, D.R. (1994) Classification of acid denaturation of proteins: Intermediates and unfolded states. *Biochemistry* **33**, 12504-12511
27. Iwakura, M. and Tanaka, T. (1992) Dihydrofolate reductase gene as a versatile expression marker. *J. Biochem.* **111**, 31-36
28. Dawson, R.M.C., Elliott, D.C., Elliot, W.H., and Jones, K.M. (1986) *Data for Biochemical Research* (3rd ed.) p. 30, Oxford University Press, New York
29. Takeda, K. and Moriyama, Y. (1991) Unavoidable time-dependent ellipticity changes of proteins in the current CD measurements. *J. Am. Chem. Soc.* **113**, 6700-6701
30. Gally, J.A. and Edelman, G.M. (1962) The effect of temperature on the fluorescence of some aromatic amino acids and proteins. *Biochim. Biophys. Acta* **60**, 499-509
31. Nakagawa, T. and Oyanagi, Y. (1980) Program system SALS for nonlinear least-squares fitting in experimental sciences in *Recent Developments in Statistical Inference and Data Analysis* (Matsushita, K., ed.) pp. 221-225, North Holland Publishing, Amsterdam
32. Ogasahara, K., Matsushita, E., and Yutani, K. (1993) Further examination of the intermediate state in the denaturation of the tryptophan synthase alpha subunit. Evidence that the equilibrium denaturation intermediate is a molten globule. *J. Mol. Biol.* **234**, 1197-1206
33. Martinez, J.C., Filimonov, V.V., Mateo, P.L., Schreiber, G., and Fersht, A.R. (1995) A calorimetric study of the thermal stability of barstar and its interaction with barnase. *Biochemistry* **34**, 5224-5233
34. Kodama, M., Takebayashi, S., and Gekko, K. (1993) Effect of amino acid-replacement on the thermal transition and stability of *E. coli* dihydrofolate reductase (in Japanese). *Nippon Kagaku Kaishi* 22-27
35. Ikeguchi, M., Kuwajima, K., Mitani, M., and Sugai, S. (1986) Evidence for identity between the equilibrium unfolding intermediate and a transient folding intermediate: A comparative study of the folding reactions of α-lactalbumin and lysozyme. *Biochemistry* **25**, 6965-6972
36. Jennings, P.A. and Wright, P.E. (1993) Formation of a molten globule intermediate early in the kinetic folding pathway of apomyoglobin. *Science* **262**, 892-896